

# Pion and muon production in $e^-, e^+, \gamma$ -plasma

Inga Kuznetsova<sup>1</sup>, Dietrich Habs<sup>2</sup> and Johann Rafelski<sup>1,2</sup>

<sup>1</sup>*Department of Physics, University of Arizona, Tucson, Arizona, 85721, USA and*

<sup>2</sup>*Department für Physik der Ludwig-Maximilians-Universität München und  
Maier-Leibnitz-Laboratorium, Am Coulombwall 1, 85748 Garching, Germany*

(Dated: May 28, 2008)

We study production and equilibration of pions and muons in relativistic electron-positron-photon plasma at a temperature  $T \ll m_\mu, m_\pi$ . We argue that the observation of pions and muons can be a diagnostic tool in the study of the initial properties of such a plasma formed by means of strong laser fields. Conversely, properties of muons and pions in thermal environment become accessible to precise experimental study.

PACS numbers: 13.60.Le, 52.27.Ny, 33.20.Xx

## I. INTRODUCTION

The formation of a relativistic (temperature  $T$  in MeV range), electron-positron-photon  $e^-, e^+, \gamma$  plasma (EP<sup>3</sup>) in the laboratory using ultra-short pulse lasers is one of the topics of current interest and forthcoming experimental effort [1, 2]. The elementary properties of EP<sup>3</sup> have recently been reported, see [3], where typical properties are explicitly presented for  $T = 10$  MeV. One of the challenges facing a study of EP<sup>3</sup> will be the understanding of the fundamental mechanisms leading to its formation. We propose here as a probe the production of heavy particles with mass  $m \gg T$ . Clearly, these processes occur during the history of the event at the highest available temperature, and thus information about the early stages of the plasma, and even pre-equilibrium state should become accessible in this way.

We focus our attention on the strongly interacting pions  $\pi^\pm, \pi^0$  ( $m_\pi c^2 \lesssim 140$  MeV), and muons  $\mu^\pm$  ( $m_\mu c^2 \lesssim 106$  MeV), (*in the following we use units in which  $k = c = \hbar = 1$  and thus we omit these symbols from all equations. Both, the particle mass, and plasma temperature, is thus given in the energy unit MeV.*) These very heavy, compared to the electron ( $m_e c^2 = 0.511$  MeV), particles are as noted natural ‘deep’ diagnostic tools of the EP<sup>3</sup> drop. Of special interest is the neutral pion  $\pi^0$  which is, among all other heavy particles, most copiously produced for  $T \ll m$ . The  $\pi^0$  yield and spectrum will be therefore of great interest in the study of the EP<sup>3</sup> properties. Conversely, the study of the in-medium pion mass splitting  $\Delta m = m_{\pi^\pm} - m_{\pi^0} = 4.594$  MeV at a temperature  $T \gtrsim \Delta m$  will contribute to the better understanding of this relatively large mass splitting between  $\pi^0$  and  $\pi^\pm$ ,  $\Delta m / \overline{m} = 3.34\%$ , believed to originate in the isospin symmetry breaking electromagnetic radiative corrections.

However, given its very short natural lifespan:

$$\pi^0 \rightarrow \gamma + \gamma, \quad \tau_{\pi^0}^0 = (8.4 \pm 0.6)10^{-17}\text{s}.$$

$\pi^0$  is also the particle most difficult to experimentally study among those we consider: its decay products reach the detection system nearly at the same time as the electromagnetic energy pulse of the decaying plasma fireball, which is likely to ‘blind’ the detectors.

This plasma drop we consider is a thousand times hotter than the center of the sun. This implies presence of the corresponding high particle density  $n$ , energy density  $\epsilon$  and pressure  $P$ . These quantities in the plasma can be evaluated using the relativistic expressions:

$$n_i = \int g_i f_i(p) d^3p, \quad (1)$$

$$\epsilon = \int \sum_i g_i E_i f_i(p) d^3p, \quad E_i = \sqrt{m_i^2 + \vec{p}^2} \quad (2)$$

$$P = \frac{1}{3} \int \sum_i g_i \left( E_i - \frac{m_i^2}{E_i} \right) f_i(p) dp^3, \quad (3)$$

where subscript  $i \in \gamma, e^-, e^+, \pi^0, \pi^+, \pi^-, \mu^-, \mu^+, f_i(p)$  is the momentum distribution of the particle  $i$  and  $g_i$  its degeneracy, for  $i = e^-, e^+, \gamma, \mu^-, \mu^+$  we have  $g_i = 2$ , and  $g_i = 1$  for  $\pi^0, \pi^-, \pi^+$ . For a QED plasma which lives long enough so that electrons, positrons are in thermal and chemical equilibrium with photons, ignoring small QED

interaction effects, we use Fermi and Bose momentum distribution, respectively:

$$f_{e^\pm} = \frac{1}{e^{(u \cdot p_e \pm \nu_e)/T} + 1}, \quad f_\gamma = \frac{1}{e^{u \cdot p_\gamma/T} - 1}, \quad (4)$$

The invariant form comprises the Lorentz-scalar  $u \cdot p_e$ , a scalar product of the particle 4-momentum  $p_i^\mu$  with the local 4-vector of velocity  $u^\mu$ . In absence of matter flow and in the rest (in the laboratory) frame we have

$$u^\mu = (1, \vec{0}), \quad p_i^\mu = (E_i, \vec{p}_i). \quad (5)$$

When the electron chemical potential  $\nu_e$  is small,  $\pi T \gg \nu_e$ , the number of particles and antiparticles is the same,  $n_{e^-} = n_{e^+}$ . Physically, it means that the number of  $e^+e^-$  pairs produced is dominating residual matter electron yield. This is the case for all laboratory experimental environments of interest here, in which  $T > 2$  MeV is achieved. We thus will set  $\nu_e = 0$  in the following.

It is convenient to parametrize the electron, positron and photon  $e^-, e^+, \gamma$  plasma properties in terms of the properties of the Stephan-Boltzmann law for massless particles (photons), presenting the physical properties in terms of the effective degeneracy  $g(T)$  comprising the count of all particles present at a given temperature  $T$ :

$$\frac{\mathcal{E}}{V} = \epsilon = g(T)\sigma T^4, \quad 3P = g'(T)\sigma T^4, \quad \sigma = \frac{\pi^2}{30}. \quad (6)$$

For temperatures  $T \ll m_e$  we only have in this case truly massless photons and  $g(T) \simeq g'(T) \simeq 2\gamma$ . Once temperature approaches and increases beyond  $m_e$  we find  $g \simeq g'(T) \simeq 2\gamma + (7/8)(2e^- + 2e^+) = 5.5$  degrees of freedom. In principle these particles acquire additional in medium mass which reduces the degree of freedom count, but this effect is compensated by collective ‘plasmon’ modes, thus we proceed with naive counting of nearly free EP<sup>3</sup> components. The factor 7/8 expresses the difference in the evaluation of Eq. (3) for the momentum distribution of Fermions and Bosons Eq. (4), with Bosons providing the reference point at low  $T$ , where only massless photons are present. In passing, we note that in the early Universe, there would be further present the neutrino degrees of freedom, not considered here for the laboratory experiments, considering their weak coupling to matter.

In figure 1 we present both  $g(T)$  and  $g'(T)$ , as a function of temperature  $T$  in form of the energy density  $\epsilon$  normalized by  $\sigma T^4$ , and, respectively, the pressure  $P$ , normalized by  $\sigma T^4/3$ . The  $g(T)$  jumps more rapidly compared to  $g'(T)$ , between the limiting case of a black body photon gas at  $T < 0.5$  MeV ( $g = 2$ ) and the case  $g = 5.5$  for  $\gamma, e^-, e^+$ , since the energy density also contains the rest mass energy content of all particles present. The rise of the ratio at  $T > 15$  MeV indicates the contribution of the excitation of muons and pions in equilibrated plasma. We note that the plasma produced pions (and muons) are in general not in chemical equilibrium. The distribution functions which maximize entropy content at given particle number and energy content are [5]:

$$f_\pi = \frac{1}{\Upsilon_{\pi^0(\pi^\pm)}^{-1} e^{u \cdot p_\pi/T} - 1}, \quad f_\mu = \frac{1}{\Upsilon_\mu^{-1} e^{u \cdot p_\mu/T} + 1}, \quad (7)$$

where  $\Upsilon_{\pi^0(\pi^\pm)}$  and  $\Upsilon_\mu$  are particles fugacities. For  $\Upsilon_i \rightarrow 0$  the quantum distributions shown in Eq. (7) turn into the classical Boltzmann distributions, with abundance prefactor  $\Upsilon_i$ .

In the case of interest here, when  $T < m$ , it suffices to consider the Boltzmann limit of the quantum distributions Eq.(7), that is to drop the ‘one’ in the denominator. Using the the Boltzmann momentum distribution and taking the non-relativistic limit we have:

$$\frac{N_\pi}{V} \equiv n_\pi = \Upsilon_\pi \frac{1}{2\pi^2} T m_\pi^2 K_2(m_\pi/T) \rightarrow \Upsilon_\pi \left( \frac{m_\pi T}{2\pi} \right)^{3/2} e^{-m_\pi/T} + \dots, \quad (8)$$

where  $K_2$  (and further below also  $K_1$ ) are the modified Bessel functions of integer order ‘2’ (and ‘1’ respectively).

The particle densities are shown on right in figure 1. The top solid line is the sum of  $n_{e^+} + n_{e^-}$ , which is marginally bigger than the photon density (dashed, blue) which follows below. We also include in the figure the sum density of muons  $n_{\mu^+} + n_{\mu^-}$  (red, dashed), and the density of the neutral pion  $\pi^0$  (bottom solid line). The chemical equilibrium corresponds to  $\Upsilon_{\pi^0(\pi^\pm)} = \Upsilon_\mu = 1$  is used in figure 1 on right, since this is the maximum density that can be reached in the buildup of these particles, for a given temperature. Both heavy particle densities appear comparatively small in the temperature range of interest. However, in magnitude they rival the normal atomic density ( $\simeq 10^2/\text{nm}^3$ ) already at  $T = 4$  MeV, and 5 MeV, respectively. This high particle density in the chemically equilibrated plasma explains the relatively large collision and reaction rates we obtain in this work. In turn, this opens the question how such dense, chemically equilibrated EP<sup>3</sup> state can be formed – we observe that colliding two ultra intense circularly polarized and

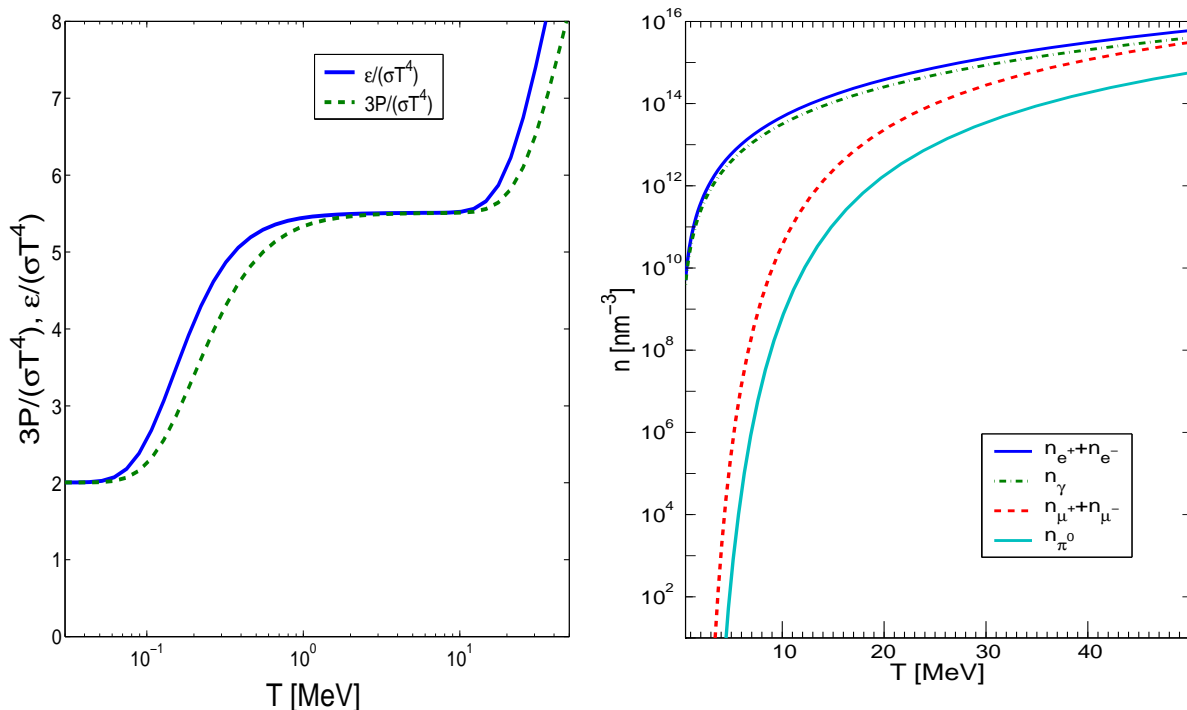


FIG. 1: On left: the ratios  $g \equiv \epsilon/\sigma T^4$  and  $g' \equiv 3P/\sigma T^4$  as a function of temperature  $T$ ; on right: the equilibrium densities of electrons (blue, solid line), photons (green, dash-dot line), muons (red, dashed line), pions (blue dotted line) as functions of temperature  $T$ .

focused laser beams on a heavy thin metal foil(s) is the current line of approach. Initial simulations were performed [4]. Many strategies can be envisaged aiming to deposit the laser pulse energy in the smallest possible spatial and temporal volume and this interesting and challenging topic will without doubt keep us and others busy in years to come.

As it turns out, even a small drop of EP<sup>3</sup> plasma with a size scale of 1nm is, given the high particle density, opaque. The mean free paths  $l_i$  of particles ‘i’ are relatively short, at sub nano-scale [3]:

$$l_e \simeq \left(\frac{10 \text{ MeV}}{T}\right)^3 \left(\frac{E}{31.1 \text{ MeV}}\right)^2 0.37 \text{ nm}, \quad l_\gamma \simeq \left(\frac{10 \text{ MeV}}{T}\right)^2 \left(\frac{E}{27.5 \text{ MeV}}\right) 0.28 \text{ nm}. \quad (9)$$

Where the reference energy values (31.1 and 27.5 MeV) correspond to the mean particle energy at  $T = 10$  MeV. Photons are subject to Compton scattering, and electrons and positrons to charged particle scattering. In fact these values of  $l_i$  are likely to be upper limits, since Bremsstrahlung type processes are believed to further increase opaqueness of the plasma [6]. In our considerations plasma particles of energy above 70 MeV are of interest, since these are responsible for the production of heavy particles. We see that the mean free path of such particles has also nm scale magnitude.

We note that a EP<sup>3</sup> drop of radius 2nm at  $T = 10$  MeV contains 13 kJ energy. This is the expected energy content of a light pulse at ELI (European Light Infrastructure, in development) with a pulse length of about  $\Delta t = 10^{-14}$ s. For comparison, the maximum energy available in particle accelerators for at least 20, if not more, years will be in head on Pb–Pb central collisions at LHC (Large Hadron Collider) at CERN, in its LHC-ion collider mode, where per nucleon energy of about 3 TeV is reached. Thus the total energy available is 200  $\mu$ J, of which about 10%–20% becomes thermalized. Thus ELI will have already an overall energy advantage of  $10^9$ , while in the LHC-ion case the great advantage are a) the natural localization of the energy at the length scale of  $10^{-5}$ nm, given that the energy is contained in colliding nuclei, and b) the high repetition rate of collisions.

As a purely academic exercise, we note that should one find a way to ‘focus’ the energy in ELI to nuclear dimensions, and scaling the energy density with  $T^4$  up from what is expected to be seen at CERN-LHC-ion ( $T < 1$ GeV), we exceed  $T = 150$  GeV, the presumed electro-weak phase boundary. Such consideration lead the authors of Refs. [1, 2] to suggest that the electro-weak transition may be achieved at some future time using ultra-short laser pulses.

Returning to present day physics, we are assuming here that  $T$  near and in MeV range is achievable in foreseeable

future, and that much higher values are obtainable in presence of pulses with  $\Delta t < 10^{-18}s$ ,  $c\Delta t < 0.3\text{nm}$ . Hence we consider production processes for  $\pi^0, \pi^\pm, \mu^\pm$  for  $T < 50$  MeV. We study here all two body reactions in EP<sup>3</sup> which lead to formation of the particles of interest, excluding solely  $e\gamma \rightarrow e\pi^0$ , and the related  $e^-e^+ \rightarrow \gamma\pi^0$ . The presence of a significant (1.2%) fraction of  $\pi^0 \rightarrow e^+e^-\gamma$  decays implies that these related two body processes could be important in our considerations. However, these reactions involve the  $\pi_0$  off-mass shell coupling to two photons, which needs to be better understood before we can consider these reactions in our context.

We also do not consider here the inverse three body reactions  $e^+e^-\gamma \rightarrow \pi^0$ , since there is no exponential gain in using  $n > 2$  particles to overcome an energy threshold, here  $m_{\pi^0}$ . The independent probability of finding  $n$  particles with energy  $m_{\pi^0}/n$  each is the same for any value of  $n$ :

$$P_1 P_2 \dots P_n \propto \left( e^{-m_{\pi^0}/nT} \right)^n = e^{-\frac{m_{\pi^0}}{T}}. \quad (10)$$

This resolves the argument that more particles could overcome more easily the reaction barrier.  $n$ -body reactions with  $n > 2$  are in fact suppressed in EP<sup>3</sup> by the weakness of the electromagnetic (EM) interaction, since adding an EM-interacting particle to the reactions process requires an EM-vertex with  $\alpha = 1/137$ . Thus microscopic reactions in EP<sup>3</sup> involving  $n > 2$  are suppressed by a factor 100 for each additional EM particle involved in the reaction. This does not mean that a collective/coherent process of heavy particle production by many particles is similarly suppressed: for example fast time varying electromagnetic fields provide through  $\vec{E} \cdot \vec{B}$  a collective source of  $\pi^0$ . We defer further study of this production mechanism which requires multi MeV<sup>-1</sup> range oscillation to be present in EP<sup>3</sup>.

In the following section, we introduce the master equation governing the production of pions and muons in plasma and formulate the invariant rates in terms of know physical reactions. In section III we obtain the numerical results for particles production rates and reactions relaxation times which we present as figures. In section IV we discuss these results further and consider their implications.

## II. PARTICLES PRODUCTION RATES

### A. $\pi^0$ production

$\pi^0$  in the QED plasma is produced predominantly in the thermal two photon fusion [7]:

$$\gamma + \gamma \rightarrow \pi^0. \quad (11)$$

Much less probable is the production of  $\pi_0$  in the reaction:

$$e^- + e^+ \rightarrow \pi^0. \quad (12)$$

These formation processes are the inverse of the decay process of  $\pi_0$ . The smallness of the electro-formation of  $\pi_0$  is characterized by the small branching ratio in  $\pi_0$  decay  $B = \Gamma_{ee}/\Gamma_{\gamma\gamma} = 6.2 \pm 0.510^{-8}$ . Other decay processes involve more than two particles.  $\pi^0$  can also be formed by charged pions in charge exchange reactions. However, in EP<sup>3</sup> in the domain of  $T$  of interest we find that at first the neutral pions will be produced. These in turn produce charged pions. Therefore we introduce the pion charge exchange process in the context of charged pion formation in the subsection II C, and since these can be important, we show these explicitly here as well.

Omitting all sub-dominant processes, the resulting master equation for neutral pion number evolution is:

$$\begin{aligned} \frac{1}{V} \frac{dN_{\pi^0}}{dt} &= \frac{d^4 W_{\gamma\gamma \rightarrow \pi^0}}{dV dt} - \frac{d^4 W_{\pi^0 \rightarrow \gamma\gamma}}{dV dt} \\ &+ \frac{d^4 W_{\pi^+\pi^- \rightarrow \pi^0 + \pi^0}}{dV dt} - \frac{d^4 W_{\pi^0 + \pi^0 \rightarrow \pi^+\pi^-}}{dV dt}, \end{aligned} \quad (13)$$

where  $N_{\pi^0}$  is total number of  $\pi^0$ ,  $V$  is volume of the system,  $d^4 W_{\gamma\gamma \rightarrow \pi^0}/dV dt$  is the (Lorentz) invariant  $\pi^0$  production rate per unit time and volume in photon fusion, and  $d^4 W_{\pi^0 \rightarrow \gamma\gamma}/dV dt$  is the invariant  $\pi^0$  decay rate per unit volume and time. Similarly,  $d^4 W_{\pi^+\pi^- \rightarrow \pi^0 + \pi^0}/dV dt$  is the pion charge exchange  $\pi^0$  production rate per unit time and volume while  $d^4 W_{\pi^0 + \pi^0 \rightarrow \pi^+\pi^-}/dV dt$  is the corresponding reverse reaction loss rate.

We assume that in the laboratory frame the momentum distribution of produced  $\pi^0$  are characterized by the ambient temperature. Eq. (8) defines the relation of fugacity  $\Upsilon_\pi$  to the yield. This equation allows now to study the production dynamics as if we were dealing with a  $\pi^0$  in a thermal bath, and to exploit the detailed balance between decay and production process in order to estimate the rate of  $\pi^0$  production. This theoretical consideration should

not be understood as assumption of equilibration of  $\pi^0$ , which could upon production escape from the small plasma drop.

In [7] the detailed balance relation is derived in detail, which takes the form

$$\Upsilon_{\pi^0}^{-1} \frac{d^4 W_{\pi^0 \rightarrow \gamma\gamma}}{dV dt} = \Upsilon_{\gamma}^{-2} \frac{d^4 W_{\gamma\gamma \rightarrow \pi^0}}{dV dt} \equiv R_{\pi^0}. \quad (14)$$

This allows that Eq.(13) can be written in the form:

$$\frac{1}{V} \frac{dN_{\pi^0}}{dt} = (\Upsilon_{\gamma}^2 - \Upsilon_{\pi^0}) R_{\pi^0} - (\Upsilon_{\pi^0}^2 - \Upsilon_{\pi^\pm}^2) R_{\pi^0 \pi^0 \leftrightarrow \pi^+ \pi^-}. \quad (15)$$

For  $\Upsilon_{\pi^0} \rightarrow \Upsilon_{\gamma}^2 \rightarrow \Upsilon_{\pi^\pm}^2 = 1$  we reach chemical equilibrium, the time variation of density due to production and decay vanishes.

The charge exchange process rate ( $R_{\pi^0 \pi^0 \leftrightarrow \pi^+ \pi^-}$ , last in Eq. (15)) balances the first contribution in Eq. (44), where it will be further discussed. The rate  $R_{\pi^0}$  can be written as

$$R_{\pi^0} = \int \frac{d^3 p_{\pi}}{(2\pi)^3 2E_{\pi}} \int \frac{d^3 p_{2\gamma}}{(2\pi)^3 2E_{2\gamma}} \int \frac{d^3 p_{1\gamma}}{(2\pi)^3 2E_{1\gamma}} (2\pi)^4 \delta^4 (p_{1\gamma} + p_{2\gamma} - p_{\pi}) \times \sum_{spin} |\langle p_{1\gamma} p_{2\gamma} | M | p_{\pi} \rangle|^2 f_{\pi}(p_{\pi}) f_{\gamma}(p_{1\gamma}) f_{\gamma}(p_{2\gamma}) \Upsilon_{\gamma}^{-2} \Upsilon_{\pi^0}^{-1} e^{u \cdot p_{\pi}/T}. \quad (16)$$

where for  $\pi^0$  formation there was the factor  $(1 + f_{\pi})$  which we reduced using the relation

$$1 \mp f_{\pm} = \Upsilon_i^{-1} e^{u \cdot p_i/T} f_{\pm}, \quad (17)$$

where Fermi ( $f_+$ ) and Bose ( $f_-$ ) distributions are implied for particle  $i$ . Similarly, in the  $\pi^0$ -decay case we replaced the two stimulated decay factors  $(1 + f_{\gamma})^2$  in that way. Eq.(16) follows Including in Eq.(16) the prefactors required by Eq.(14) and recalling time reversal invariance, i.e.  $M = M^\dagger$ :

$$|\langle p_{1\gamma} p_{2\gamma} | M | p_{\pi} \rangle|^2 = |\langle p_{\pi} | M | p_{1\gamma} p_{2\gamma} \rangle|^2. \quad (18)$$

We realize that the result, Eq.(16) is manifestly symmetric for the two reaction directions. It is interesting to note that in Boltzmann limit all fugacities cancel in Eq.(16).

We introduce the pion equilibration (relaxation) time constant by:

$$\tau_{\pi^0} = \frac{dn_{\pi^0}/d\Upsilon_{\pi^0}}{R_{\pi^0}}. \quad (19)$$

Note that when the volume does not change in time on scale of  $\tau_{\pi^0}$  (absence of expansion dilution) and thus  $T$  is constant, the left hand side of Eq.(15) becomes  $dn_{\pi^0}/dt$ . Given the relaxation time definition Eq.(19) the time evolution for of the pion fugacity for a system at fixed time independent temperature satisfies:

$$\tau_{\pi^0} \frac{d\Upsilon_{\pi^0}}{dt} = \Upsilon_{\gamma}^2 - \Upsilon_{\pi^0} - (\Upsilon_{\pi^0}^2 - \Upsilon_{\pi^\pm}^2) \frac{R_{\pi^0 \pi^0 \leftrightarrow \pi^+ \pi^-}}{R_{\pi^0}}. \quad (20)$$

When the charge exchange reaction can be ignored, for  $\Upsilon_{\pi^0}(t=0) = 0$  we find the analytical solution  $\Upsilon_{\pi^0} = \Upsilon_{\gamma}^2 (1 - e^{-t/\tau_{\pi^0}})$ , justifying the proposed definition of the relaxation constant.

We note that Eq.(20) also describes the decay of a  $\pi^0$ . Therefore, up to small modifications introduced by the thermal medium (see discussion below),

$$\tau_{\pi^0} \simeq \tau_{\pi^0}^0.$$

The  $\pi^0$  production rate is thus related to the decay rate  $1/\tau_{\pi^0}^0$  by the simple formula

$$R_{\pi^0} \simeq \frac{dn_{\pi^0}/d\Upsilon_{\pi^0}}{\tau_{\pi^0}^0} \simeq \left( \frac{m_{\pi} T}{2\pi} \right)^{3/2} \frac{e^{-m_{\pi}/T}}{\tau_{\pi^0}^0}, \quad (21)$$

where in the last expression we have used Eq.(8) in the limit  $m \gg T$ . It is important for the reader to remember that derivation of Eq (21) is based on detailed balance in thermally equilibrated plasma, and does not require chemical equilibrium to be established.

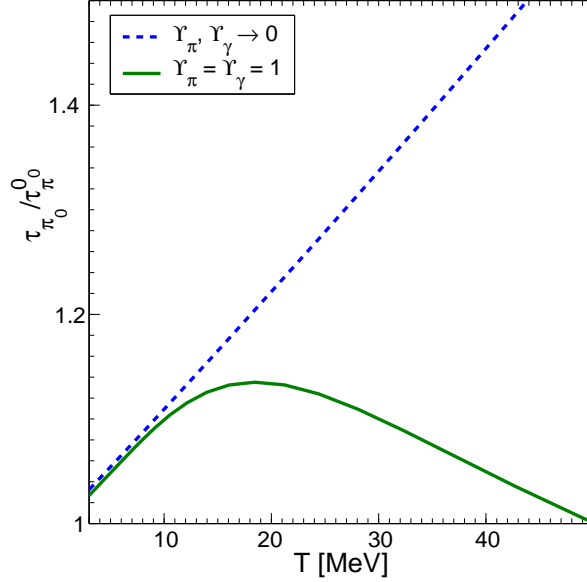


FIG. 2: The ratios  $\tau_{\pi^0}/\tau_{\pi^0}^0$  as functions of temperature  $T$  for relativistic Boltzmann limit (blue, dashed line) and for quantum distribution in chemical equilibrium,  $\Upsilon_{\pi} = \Upsilon_{\gamma} = 1$  (green, solid line).

Now we consider how and why  $\tau_{\pi^0} \simeq \tau_{\pi^0}^0$ . It turns out that there are both relativistic and quantum effects which contribute and they (nearly) cancel: the relativistic effect arises because  $\tau_{\pi^0}$  in Eq.(21) is in lab frame while the known  $\tau_{\pi^0}^0$  is in the pion rest frame. In the relativistic Boltzmann limit the correction is obtained considering the related time dilation effect [7] is:

$$\tau_{\pi^0} = \frac{\tau_{\pi^0}^0}{\langle 1/\gamma \rangle} = \tau_{\pi^0}^0 \frac{K_2(m_{\pi^0}/T)}{K_1(m_{\pi^0}/T)}, \quad (22)$$

where  $\langle 1/\gamma \rangle$  is average inverse Lorentz factor. We find that this effect implies that  $\tau_{\pi^0}$  in the lab frame increases with temperature. This effect is shown by dashed (blue) line in figure 2. Furthermore, with increasing temperature quantum distribution functions for photons and for the produced particle need to be considered. This leads to the result shown as solid line (green) in figure 2. Thus in general  $\tau_{\pi^0} > \tau_{\pi^0}^0$ , by up to 14%.

We can further evaluate exactly the reaction rate Eq.(16) [7]:

$$R_{\pi^0} = \frac{1}{(2\pi)^2} \frac{m_{\pi}}{\tau_{\pi^0}^0} \int_0^{\infty} \frac{p_{\pi}^2 dp_{\pi}}{E_{\pi}} \frac{\Upsilon_{\pi^0}^{-1} e^{E_{\pi}/T}}{\Upsilon_{\pi^0}^{-1} e^{E_{\pi}/T} - 1} \Phi(p_{\pi}), \quad (23)$$

where

$$\Phi(p_{\pi}) = \int_{-1}^1 d\zeta \Upsilon_{\gamma}^{-2} \frac{1}{\Upsilon_{\gamma}^{-1} e^{(a-b\zeta)} - 1} \frac{1}{\Upsilon_{\gamma}^{-1} e^{(a+b\zeta)} - 1}, \quad (24)$$

with

$$a = \frac{\sqrt{m_{\pi}^2 + p_{\pi}^2}}{2T}; \quad b = \frac{p_{\pi}}{2T}. \quad (25)$$

This integral for  $\Upsilon_{\gamma} = 1$  takes the form:

$$\Phi(p_{\pi^0}) = \frac{2}{b(e^{2a} - 1)} \left( b + \ln \left( 1 + \frac{(e^{(b-a)} - e^{-(a+b)})}{(1 - e^{b-a})} \right) \right). \quad (26)$$

This exact result (blue, solid line) is compared to the approximate result Eq.(21) (green, dashed line) in figure 3. We note that it is hard to discern a difference on logarithmic scale, especially so for small temperatures where the only

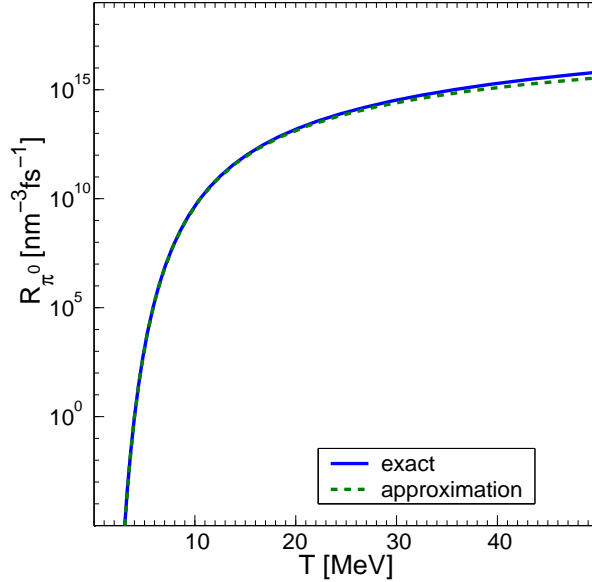


FIG. 3: The  $\pi_0$  production rate (blue, solid line) and approximate rate from Eq.(21) (green dashed line) as functions of temperature  $T$ .

(small) effect is the relativistic time dilation. This implies that it is appropriate to use the simple result Eq.(21) in the study of  $\pi^0$  production.

Before closing this section we note that we can use exactly the same method to extract from the partial width of the  $\pi_0 \rightarrow e^+e^-$  the reaction rate for the inverse process, which will be discussed below. All arguments carry through in identical and exact fashion replacing where appropriate the Bose by Fermi distributions and using Eq.17.

## B. Muon production

In the plasma under consideration, muons can be directly produced in the reactions:

$$\gamma + \gamma \rightarrow \mu^+ + \mu^-, \quad (27)$$

$$e^+ + e^- \rightarrow \mu^+ + \mu^-. \quad (28)$$

For reactions (27) and (28) the master evolution equation developed for the study of thermal strangeness in heavy ion collisions applies [8, 9, 10, 11] (compared to these references our definition is changed, their  $R_{12 \rightarrow 34} \rightarrow R_{12 \rightarrow 34}/(\Upsilon_1 \Upsilon_2)$  in order to make the forward-backward symmetry explicit )

$$\frac{1}{V} \frac{dN_\mu}{dt} = (\Upsilon_\gamma^2 - \Upsilon_\mu^2) R_{\gamma\gamma \leftrightarrow \mu^+\mu^-} + (\Upsilon_e^2 - \Upsilon_\mu^2) R_{e^+e^- \leftrightarrow \mu^+\mu^-}. \quad (29)$$

Like before for  $\pi^0$  we consider the master equation in order to find appropriate definition of the relaxation time constant for  $\mu^\pm$  production. In no way should this be understood to imply that muons are retained in the small plasma drop. In chemically equilibrated EP<sup>3</sup> the  $\mu$  production relaxation time is defined by:

$$\tau_\mu = \frac{1}{a} \frac{dn_\mu/d\Upsilon_\mu}{(R_{\gamma\gamma \leftrightarrow \mu^+\mu^-} + R_{e^+e^- \leftrightarrow \mu^+\mu^-})}, \quad (30)$$

where a suitable choice is  $a = 1, 2$  for  $t = 0, \infty$ , respectively (see below). The form of Eq. (30) assures that, omitting the volume expansion, i.e. the dilution effect, the evolution of the muon fugacity obeys the equation

$$a\tau_\mu \frac{d\Upsilon_\mu}{dt} = 1 - \Upsilon_\mu^2, \quad \Upsilon_\gamma = \Upsilon_e = 1, \quad (31)$$

which has for  $\Upsilon_\mu(t=0) = 0$  the simple analytical solution [9]:

$$\Upsilon_\mu = \tanh t/a\tau_\mu. \quad (32)$$

For  $t \rightarrow \infty$ , near to chemical equilibrium,  $\Upsilon_\mu \rightarrow 1 - e^{-2t/a\tau_\mu}$ , while for  $t \rightarrow 0$ , at the onset of particle production with small  $\Upsilon_\mu$  we have  $\Upsilon_\mu = t/(a\tau_\mu)$ . Hence, near to chemical equilibrium it is appropriate to use  $a = 2$  in definition of relaxation time Eq.(30), while at the onset of particle production, more applicable to this work a more physical choice would be  $a = 1$ . However, following the convention, in the results presented below the value  $a = 2$  is used.

The invariant muon production rate in photon fusion as introduced above is:

$$R_{\gamma\gamma \leftrightarrow \mu^+\mu^-} = \int \frac{d^3 p_{\mu^+}}{(2\pi)^3 2E_{\mu^+}} \int \frac{d^3 p_{\mu^-}}{(2\pi)^3 2E_{\mu^-}} \int \frac{d^3 p_{1\gamma}}{(2\pi)^3 2E_{1\gamma}} \int \frac{d^3 p_{2\gamma}}{(2\pi)^3 2E_{2\gamma}} (2\pi)^4 \delta^4(p_{1\gamma} + p_{2\gamma} - p_{\mu^+} - p_{\mu^-}) \times \sum_{\text{spin}} |\langle p_{1\gamma} p_{2\gamma} | M_{\gamma\gamma \rightarrow \mu^+\mu^-} | p_{\mu^+} p_{\mu^-} \rangle|^2 f_\gamma(p_{1\gamma}) f_\gamma(p_{2\gamma}) f_\mu(p_{\mu^+}) f_\mu(p_{\mu^-}) \Upsilon_\gamma^{-2} \Upsilon_\mu^{-2} e^{u \cdot (p_{\mu^+} + p_{\mu^-})/T} \quad (33)$$

and the invariant muon production rate in electron-positron fusion is:

$$R_{e^+e^- \leftrightarrow \mu^+\mu^-} = \int \frac{d^3 p_{\mu^+}}{(2\pi)^3 2E_{\mu^+}} \int \frac{d^3 p_{\mu^-}}{(2\pi)^3 2E_{\mu^-}} \int \frac{d^3 p_{e^+}}{(2\pi)^3 2E_{e^+}} \int \frac{d^3 p_{e^-}}{(2\pi)^3 2E_{e^-}} (2\pi)^4 \delta^4(p_{e^+} + p_{e^-} - p_{\mu^+} - p_{\mu^-}) \times \sum_{\text{spin}} |\langle p_{e^+} p_{e^-} | M_{e^+e^- \rightarrow \mu^+\mu^-} | p_{\mu^+} p_{\mu^-} \rangle|^2 f_e(p_{e^+}) f_e(p_{e^-}) f_\mu(p_{\mu^+}) f_\mu(p_{\mu^-}) \Upsilon_e^{-2} \Upsilon_\mu^{-2} e^{u \cdot (p_{\mu^+} + p_{\mu^-})/T}. \quad (34)$$

We note that in Eq. (33) and Eq. (34) in the Boltzmann limit all fugacities cancel, and that the forward-backward reaction symmetry is explicit. Moreover, it is interesting to note that despite inclusion of quantum effects (Bose stimulated emission and/or Fermi blocking), when using rates as defined in this paper, we don't change the master population equation system arising for Boltzmann particles. The only modification is a slight fugacity dependence of rates presented in Eq. (16), Eq. (33), Eq. (34).

The  $\sum |M_{e^+e^- \rightarrow \mu^+\mu^-}|^2$  differs from often considered heavy quark production  $\sum |M_{q\bar{q} \rightarrow c\bar{c}}|^2$  [12, 13] ( $m_c \gg m_q$ ) by color factor  $2/9$ , and the coupling  $\alpha_s \rightarrow \alpha$  of QCD has to be changed to  $\alpha = 1/137$  of QED. Then we obtain, based on above references:

$$\sum |M_{e^+e^- \rightarrow \mu^+\mu^-}|^2 = g_e^2 8\pi^2 \alpha^2 \frac{(m^2 - t)^2 + (m^2 - u)^2 + 2m^2 s}{s^2}, \quad (35)$$

where  $m = 106$  MeV is the muon mass, electron and positron degeneracy  $g_e = 2$ , and  $s, t, u$  are the usual Mandelstam variables:  $s = (p_1 + p_2)^2$ ,  $t = (p_3 - p_1)^2$ ,  $u = (p_3 - p_2)^2$ ,  $s + t + u = 2m^2$ . For the total averaged over initial states  $|M|^2$  for photon fusion we have

$$|M_{\gamma\gamma \rightarrow \mu^+\mu^-}|^2 = g_\gamma^2 8\pi^2 \alpha^2 \left( -4 \left( \frac{m^2}{m^2 - t} + \frac{m^2}{m^2 - u} \right)^2 + 4 \left( \frac{m^2}{m^2 - t} + \frac{m^2}{m^2 - u} \right) + \frac{m^2 - u}{m^2 - t} + \frac{m^2 - t}{m^2 - u} \right), \quad (36)$$

where degeneracy  $g_\gamma = 2$ . Near threshold  $s \approx 4m^2$ , with  $t, u \approx -m^2$  we find

$$|M_{\gamma\gamma \rightarrow \mu^+\mu^-}|^2 = 64\pi^2 \alpha^2, \quad |M_{e^+e^- \rightarrow \mu^+\mu^-}|^2 = 32\pi^2 \alpha^2. \quad (37)$$

The  $e^+e^- \rightarrow \mu^+\mu^-$  reaction involves a single photon, and thus it is more constrained (by factor 2) compared to the photon fusion, which is governed by two Compton type Feynman diagrams. However, in the rate we compute below, the indistinguishability of the two photons introduces an additional factor  $1/2$ , so that both reactions differ only by the difference in the quantum Bose and Fermi distributions.

Integrals in Eq.(33) and (34) can be evaluated in spherical coordinates. We define:

$$q = p_1 + p_2; \quad p = \frac{1}{2}(p_1 - p_2); \quad q' = p_3 + p_4; \quad p' = \frac{1}{2}(p_3 - p_4); \quad (38)$$

z-axis is chosen in the direction of  $\vec{q} = \vec{p}_1 + \vec{p}_2$ :

$$q_\mu = (q_0, 0, 0, 0), \quad p_\mu = (p_0, p \sin \theta, 0, p \cos \theta), \quad p'_\mu = (p'_0, p' \sin \phi \sin \chi, p' \sin \phi \cos \chi, p' \cos \phi).$$



Now we obtain [10]:

$$\begin{aligned}
R_{e^+e^-(\gamma\gamma)\leftrightarrow\mu^+\mu^-} &= \frac{1}{1+I} \frac{(4\pi)(2\pi)}{(2\pi)^4 16} \int_{2m_\mu}^\infty dq_0 \int_0^{s-q_0^2} dq \int_{-\frac{q}{2}}^{\frac{q}{2}} dp_0 \int_{-\frac{q^*}{2}}^{\frac{q^*}{2}} dp'_0 \int_0^\infty dp \int_0^\infty dp' \int_{-1}^1 d(\cos\theta) \int_{-1}^1 d(\cos\phi) \\
&\times \int_0^{2\pi} d\chi \delta\left(p - \left(p_0^2 + \frac{s}{4}\right)^{1/2}\right) \delta\left(p' - \left(p_0'^2 - m_\mu^2 + \frac{s}{4}\right)^{1/2}\right) \delta\left(\cos\theta - \frac{q_0 p_0}{qp}\right) \delta\left(\cos\phi - \frac{q'_0 p'_0}{qp}\right) \\
&\times \sum |M_{e^+e^-(\gamma\gamma)\rightarrow\mu\mu}|^2 \Upsilon_\mu^{-2} f_\mu\left(\frac{q_0}{2} + p_0\right) f_\mu\left(\frac{q_0}{2} - p_0\right) \Upsilon_{e(\gamma)}^{-2} f_{e(\gamma)}\left(\frac{q_0}{2} + p'_0\right) f_{e(\gamma)}\left(\frac{q_0}{2} - p'_0\right) \exp(q_0/T), \quad (39)
\end{aligned}$$

where  $q^* = q\sqrt{1 - \frac{m_\mu^2}{s}}$ . The integration over  $p, p', \cos\theta, \cos\phi$  can be done analytically considering the delta-functions. The other integrals can be evaluated numerically. For the case of indistinguishable colliding particles (two photons) there is additional factor 1/2 implemented by the value  $I = 1$ , while for distinguishable colliding particles (here electron and positron)  $I = 0$ .

### C. $\pi^\pm$ production

$\pi^\pm$  can be produced in  $\pi_0\pi_0$  charge exchange scattering:

$$\pi^0 + \pi^0 \rightarrow \pi^+ + \pi^-, \quad (40)$$

as well as in two photon, and in electron-positron fusion processes

$$\gamma + \gamma \rightarrow \pi^+ + \pi^-, \quad (41)$$

$$e^+ + e^- \rightarrow \pi^+ + \pi^-. \quad (42)$$

We find that for  $\pi^\pm$  production, the last two processes are much slower compared to the first, in case that  $\pi_0$  density is near chemical equilibrium. Similarly, the two photon fusion to two  $\pi^0$ :

$$\gamma + \gamma \rightarrow \pi^0 + \pi^0, \quad (43)$$

turns out, as expected, to be much smaller than one  $\pi^0$  production. It is a reaction of higher order in  $\alpha$  and the energy is shared between two final particles.

The time evolution equations for the number of  $\pi^\pm$  are similar to Eq. (29):

$$\frac{1}{V} \frac{dN_{\pi^\pm}}{dt} = (\Upsilon_{\pi^0}^2 - \Upsilon_{\pi^\pm}^2) R_{\pi^0\pi^0\leftrightarrow\pi^+\pi^-} + (\Upsilon_\gamma^2 - \Upsilon_{\pi^\pm}^2) R_{\gamma\gamma\leftrightarrow\pi^+\pi^-} + (\Upsilon_e^2 - \Upsilon_{\pi^\pm}^2) R_{e^+e^-\leftrightarrow\pi^+\pi^-}. \quad (44)$$

In order to evaluate the pion production rates in two body processes we use reaction cross section, and the relation [14]:

$$R_{12\leftrightarrow\pi^+\pi^-} = \frac{g_1 g_2}{32\pi^4} \frac{T}{1+I} \int_{s_{th}}^\infty ds \sigma(s) \frac{\lambda_2(s)}{\sqrt{s}} K_1(\sqrt{s}/T), \quad (45)$$

(compared to reference [14] our definition is changed  $R_{12\rightarrow 34} \rightarrow R_{12\rightarrow 34}/(\Upsilon_1\Upsilon_2)$ ) where

$$\lambda_2(s) = (s - (m_1 + m_2)^2)(s - (m_1 - m_2)^2), \quad (46)$$

$m_1$  and  $m_2, g_1$  and  $g_2, \Upsilon_1$  and  $\Upsilon_2$  are masses, degeneracy and fugacities of initial interacting particles.

For the respective three cross sections we use, all results valid in the common range  $s \leq 1$  GeV<sup>2</sup> we consider here:

- The cross section for charge exchange  $\pi^0$  scattering reaction Eq.(40) have been considered in depth recently [15]:

$$\sigma = \frac{16\pi}{9} \sqrt{\frac{s - 4M_{\pi^\pm}^2}{s - 4M_{\pi^0}^2}} (a_0^{(0)} - a_0^{(2)})^2; \quad (47)$$

where  $a_0^{(0)} - a_0^{(2)} = 0.27/M_{\pi^\pm}$  This is the dominant process for charge pion production, subject to presence of  $\pi^0$ .

- For process Eq.(41), the cross section of  $\pi^\pm$  production in photon fusion we use [16]:

$$\sigma_{\gamma\gamma\rightarrow\pi^+\pi^-} = \frac{2\pi\alpha^2}{s} \left(1 - \frac{4m_\pi^2}{s}\right)^{1/2} \left(\frac{m_V^4}{(1/2s + m_V^2)(1/4s + m_V^2)}\right), \quad (48)$$

where  $m_V = 1400.0$  MeV. As we will see from numerical calculations given the cross sections for  $\gamma\gamma \rightarrow \pi^+\pi^-$  resulting production rates will be smaller than the charge exchange  $\pi^0\pi^0 \rightarrow \pi^+\pi^-$  reaction.

- For process Eq.(42), the cross section of  $\pi^\pm$  production in electron - positron fusion we use [17]:

$$\sigma_{e^+e^-\rightarrow\pi^+\pi^-} = \frac{\pi\alpha^2}{3} \frac{(s - 4m_\pi^2)^{3/2}}{s^{5/2}} |F(s)|^2. \quad (49)$$

The form factor  $F(s)$  can be written in the form:

$$F(s) = \frac{m_\rho^2 + m_\rho\Gamma_\rho d}{m_\rho^2 - s + \Gamma_\rho(m_\rho^2/k_\rho^3)[k^2(h(s) - h(m_\rho^2)) + k_\rho^2 h'(m_\rho^2)(m_\rho^2 - s)] - im_\rho(k/k_\rho)^3\Gamma_\rho(m_\rho/\sqrt{s})}; \quad (50)$$

where  $h'(s) = dh/ds$  and

$$k = \left(\frac{1}{4}s - m_\pi^2\right)^{1/2}; \quad k_\rho = \left(\frac{1}{4}m_\rho^2 - m_\pi^2\right)^{1/2}; \quad h(s) = \frac{2}{\pi} \frac{k}{\sqrt{s}} \ln\left(\frac{\sqrt{s} + 2k}{2m_\pi}\right);$$

$m_\rho = 775$  MeV,  $\Gamma_\rho = 130$  MeV,  $d = 0.48$ . Given this cross section we also find that the rate of charged pion production is small when compared to  $\pi_0$ -charge exchange scattering.

- For reaction (43) we have [18]:

$$\sigma(\gamma\gamma \rightarrow \pi^0\pi^0) = \left(\frac{\alpha^2\sqrt{s - 4m_\pi^2}}{8\pi^2\sqrt{s}}\right) \left[1 + \frac{m_\pi^2}{s}f_s\right] \sigma(\pi^+\pi^- \rightarrow \pi^0\pi^0), \quad (51)$$

where

$$f_s = 2(\ln^2(z_+/z_-) - \pi^2) + \frac{m_\pi^2}{s}(\ln^2(z_+/z_-) + \pi^2)^2, \quad (52)$$

and  $z_\pm = (1/2)(1 \pm \sqrt{s - 4m_\pi^2})$ .

The cross sections for  $\pi^+\pi^-$  pair production, evaluated using Eqs.(47), (48) and (49) are presented in figure 4 as functions of reaction energy  $\sqrt{s}$ . Top solid line (blue) is for charged pions production in  $\pi^0$  scattering Eq.(40), the magnitude of this cross section being very large we reduce it in presentation by factor 1000; the dashed line is for  $\pi^+\pi^-$  production in photon fusion Eq.(41); dash-dotted line is for electron positron fusion Eq.(42). The bottom solid line (green) is for photon fusion into two neutral pions, Eq.(51). The prediction for  $\sigma_{\gamma\gamma\rightarrow\pi^+\pi^-}$  is about 480 nb (data 420 nb) at the peak near threshold [18], which is in agreement with calculations presented here. The reaction  $\sigma_{\gamma\gamma\rightarrow\pi^0\pi^0}$ (Eq.(43)) is much smaller than others and we do not consider this reaction further. We note that some of these results are currently under intense theoretical discussion as they relate to chiral symmetry. For our purposes the level of precision of here presented reaction cross sections is quite adequate.

### III. NUMERICAL RESULTS

#### A. Particle production relaxation times

In figure 5 we show relaxation time  $\tau$  for the different processes considered as function of temperature  $T \in [3, 50]$  MeV. Because of the large difference in production rates which can be compensated by different densities of particles present (magnitudes of fugacities) we introduce partial relaxation time for each of the three reactions  $\pi^0\pi^0 \rightarrow \pi^+\pi^-$ ,  $\gamma\gamma \rightarrow \pi^+\pi^-$  and  $e^+ + e^- \rightarrow \pi^+\pi^-$ :

$$\tau_{\pi^0\pi^0\leftrightarrow\pi^+\pi^-} = \frac{1}{2} \frac{dn_{\pi^\pm}/d\Upsilon_{\pi^\pm}}{R_{\pi^0\pi^0\leftrightarrow\pi^+\pi^-}}; \quad \tau_{\gamma\gamma\leftrightarrow\pi^+\pi^-} = \frac{1}{2} \frac{dn_{\pi^\pm}/d\Upsilon_{\pi^\pm}}{R_{\gamma\gamma\leftrightarrow\pi^+\pi^-}}; \quad \tau_{e^+e^-\leftrightarrow\pi^+\pi^-} = \frac{1}{2} \frac{dn_{\pi^\pm}/d\Upsilon_{\pi^\pm}}{R_{e^+e^-\leftrightarrow\pi^+\pi^-}}. \quad (53)$$

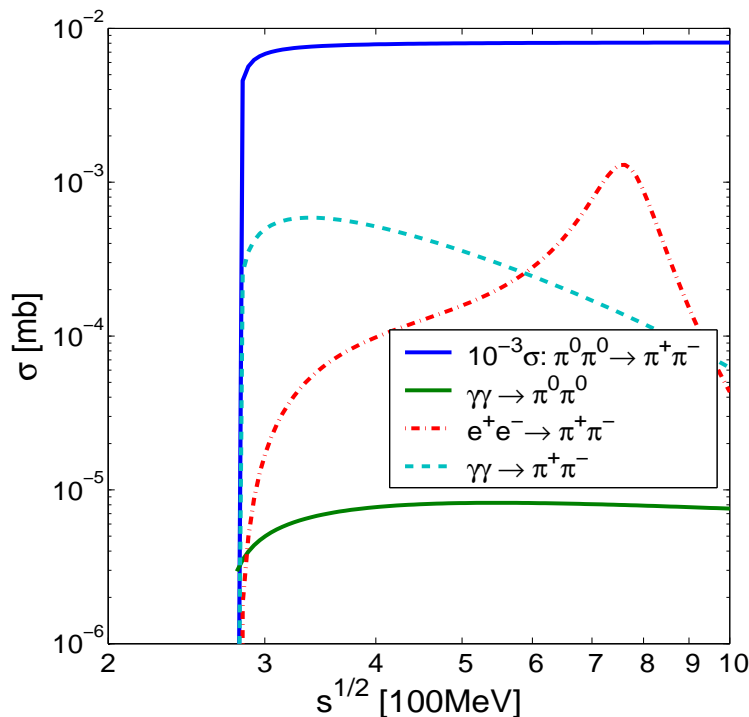


FIG. 4: The cross section  $\sigma$  for pion pair production, and pion charge exchange (solid top line), as functions of  $\sqrt{s} \leq 1 \text{ GeV}^2$ .

When  $T \ll m$ , we can use the Boltzmann approximation to the particle distribution functions. Since in this limit the density is proportional to  $\Upsilon$  the relaxation times doesn't depend on  $\Upsilon$ . Moreover, even for  $T \rightarrow 50 \text{ MeV}$ , we have for muons  $e^{-m/T} \simeq 1/3$ , thus quantum correlations in phase space remain small, and the Boltzmann limit can be employed. To account for small deviation from Boltzmann limit arising towards the upper limit of the temperature range we consider, that is at  $T \simeq 50 \text{ MeV}$ , we used the exact equations with  $\Upsilon_i = 1$  to calculate  $\tau$  for each case, value corresponding to the maximum density that can be reached for a given temperature, for which the quantum effect is largest. In addition to these three cases Eq.(53) we show in figure 5 the muon production relaxation time Eq.(30), the two photon fusion into  $\pi^0$  relaxation time Eq.(19), a nearly horizontal line (turquoise, bottom), which is slightly greater than the free space  $\pi^0$  decay rate. Finally, the thin dash-dot line at about  $10^8$  times greater value of time is the electron-positron fusion into  $\pi^0$ , Eq.(12).

### B. Rates of pion and muon formation

In figure 6 we show on left as a solid (blue) line as a function of fireball temperature the rate per unit volume and time for the process  $\gamma + \gamma \rightarrow \pi^0$ , the dominant mechanism of pion production. The other solid line with dots corresponds to  $e^+ + e^- \rightarrow \pi^0$  reaction which in essence remains, in comparison, insignificant. Its importance follows from the fact that it provides the second most dominant path to  $\pi_0$  formation at lowest temperatures considered, and it operates even if and when photons are not confined to remain in the plasma drop.

We improve the rate presentation on the right hand side in figure 6: considering that the formation of a plasma state involves an experimentally given fireball energy content  $\mathcal{E}$  in Joules, we use Eq.(6) to eliminate the volume  $V$  at each temperature  $T$ :

$$R'_{\pi^0} \equiv \frac{d^2 W'_{\gamma\gamma \rightarrow \pi^0}}{dt d\mathcal{E}} = \frac{1}{g\sigma T^4} \frac{d^4 W_{\gamma\gamma \rightarrow \pi^0}}{dV dt} = \frac{1}{g\sigma T^4} R_{\pi^0} \quad (54)$$

For chemical nonequilibrium, replace  $g \rightarrow \Upsilon_\gamma^2 g(\Upsilon)$ . Considering the (good) approximate Eq.(21) we obtain:

$$R'_{\pi^0} \simeq \left( \frac{m_\pi}{2\pi T} \right)^{3/2} \frac{e^{-m_\pi/T}}{g\sigma T \tau_{\pi^0}^0}. \quad (55)$$

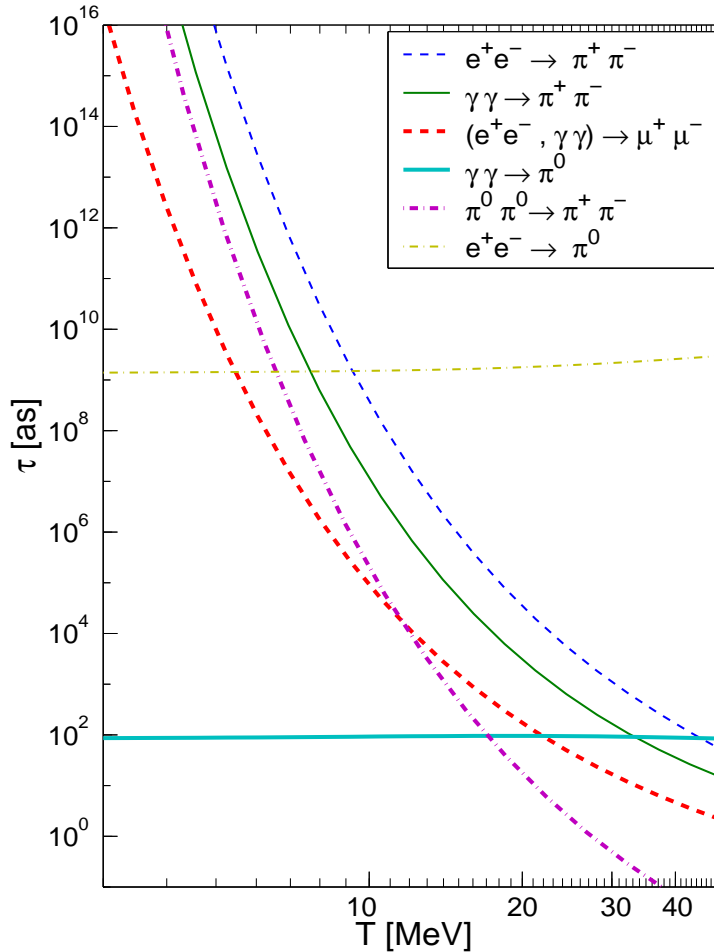


FIG. 5: The relaxation time  $\tau$  for the different channels of pion and muon production (see box), as functions of plasma temperature  $T$ .

We use units such that  $\hbar = c = k = 1$  and thus  $R'$  is a dimensionless expression. Recalling the value of these constants, the units we used for  $R'$  derive from  $\text{MeV s} = 1.603 \cdot 10^{-4} \text{ MJ fs}$ .

The other lines in figure 6 address the sum of formation rates of charged pion pairs (dashed, red) by all reactions considered in this work,  $\pi^0 + \pi^0 \rightarrow \pi^+ + \pi^-$ ,  $\gamma + \gamma \rightarrow \pi^+ + \pi^-$ ,  $e^+ + e^- \rightarrow \pi^+ + \pi^-$ . We also present the sum of all reactions leading to either a charged pion pair, or muon pair (dot-dashed, green) lines, that is adding in  $\gamma + \gamma \rightarrow \mu^+ + \mu^-$ ,  $e^+ + e^- \rightarrow \mu^+ + \mu^-$ . The rationale for this presentation is that we do not care how a heavy particle is produced, as long as it can be observed. The dashed (red) line assumes that we specifically look for charged pions, and dot-dashed (green) line that we wait till charged pions decays, being interested in the total final muon yield. The  $\pi^0$  production rate (blue, solid line) is calculated using Eq.(16) and yields on the logarithmic scale nearly indistinguishable result from the approximation Eq.(21). For  $\pi^\pm$  production we refer to section II C and for  $\mu^\pm$  production we refer to II B.

In table I we show the values of key reaction rates  $R$  and relaxation times  $\tau$  at  $T = 5$  and  $15 \text{ MeV}$ . We note the extraordinarily fast rise of the rates with temperature, in some instances bridging  $15 - 20$  orders in magnitude when results for  $T = 5$  and  $15 \text{ MeV}$  are compared.

In order to understand the individual contributions to the different reactions entering the sum of rates presented above, we show as a function of temperature in the figure 7 the relative strength of muon pair (left) and charge pion (on right) electromagnetic ( $\gamma + \gamma$ ,  $e^+ + e^-$ ) production, using as the reference the  $\gamma + \gamma \rightarrow \pi^0$  reaction. The  $\mu^\pm$  production rates are calculated using Eq.(39) with  $|M|^2$  from Eq.(35) and Eq.(36) respectively. This ratio is smaller than unity for  $T \lesssim 20 \text{ MeV}$ . For larger  $T$ , the muon direct production rate becomes larger than  $\pi^0$  production rate.

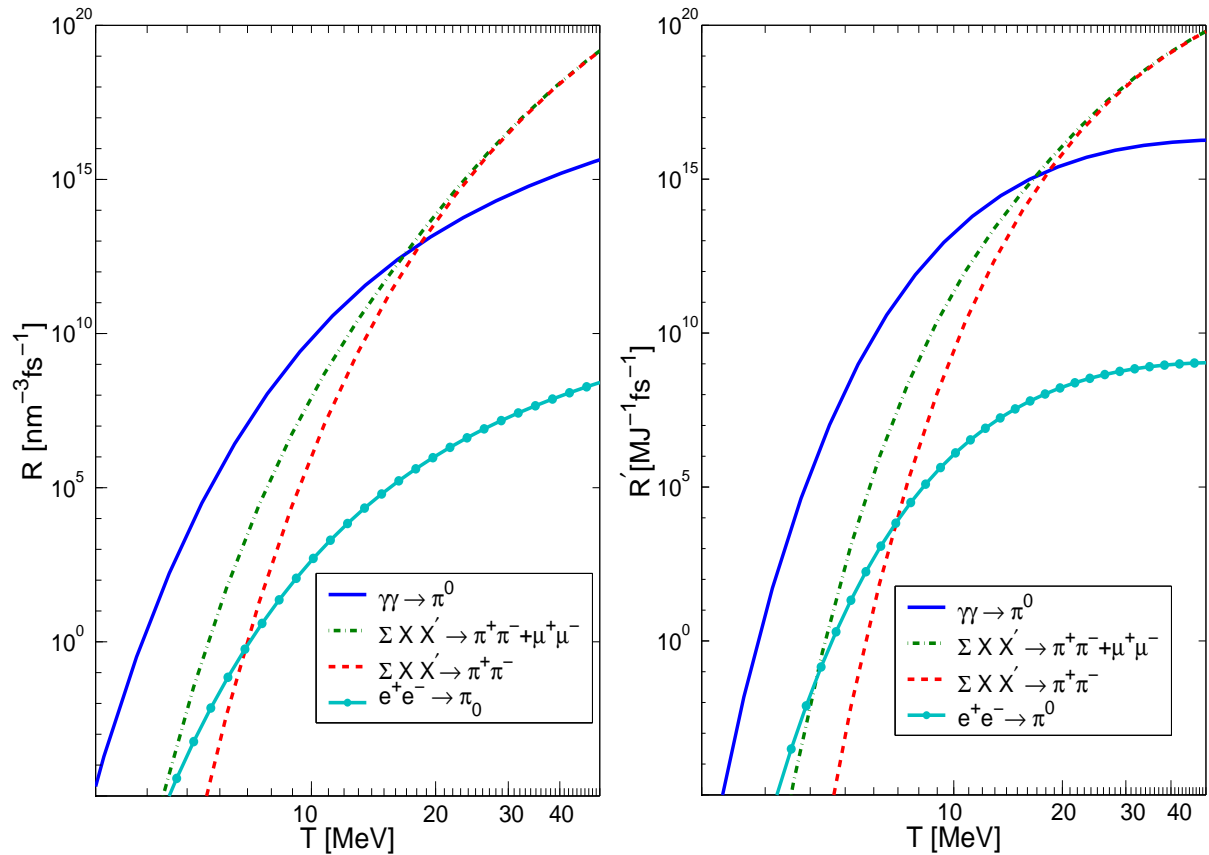


FIG. 6: On left, the invariant pion production rates in units of  $\text{nm}^{-3}\text{fs}^{-1}$ , as a function of temperature  $T$ . On right the production rate  $R'$  per Joule energy content in the fireball, in units of  $\text{MJ}^{-1}\text{fs}^{-1}$ , in both cases for reactions shown in the box.

TABLE I: Values of rates, relaxation times for all reactions at  $T = 5$  MeV and  $T = 15$  MeV

reaction	$T = 5$ MeV $\tau$ [as]	$T = 5$ MeV $R$ [ $\text{nm}^{-3}\text{fs}^{-1}$ ]	$T = 15$ MeV $\tau$ [as]	$T = 15$ MeV $R$ [ $\text{nm}^{-3}\text{fs}^{-1}$ ]
$\gamma\gamma \leftrightarrow \pi_0$	88	$3.3 \cdot 10^3$	95	$1.2 \cdot 10^{12}$
$e^+e^- \leftrightarrow \mu^+\mu^-$	$1.2 \cdot 10^{10}$	$3.2 \cdot 10^{-3}$	$1.9 \cdot 10^3$	$1.5 \cdot 10^{11}$
$\gamma\gamma \leftrightarrow \mu^+\mu^-$	$1.0 \cdot 10^{10}$	$3.7 \cdot 10^{-3}$	$1.3 \cdot 10^3$	$2.1 \cdot 10^{11}$
$\pi^0\pi^0 \leftrightarrow \pi^+\pi^-$	$2.9 \cdot 10^{12}$	$2.1 \cdot 10^{-8}$	$4.6 \cdot 10^2$	$9.5 \cdot 10^{10}$
$\gamma\gamma \leftrightarrow \pi^+\pi^-$	$6.4 \cdot 10^{13}$	$9.7 \cdot 10^{-10}$	$5.1 \cdot 10^4$	$8.7 \cdot 10^8$
$e^+e^- \leftrightarrow \pi^+\pi^-$	$7.8 \cdot 10^{15}$	$7.9 \cdot 10^{-12}$	$9.5 \cdot 10^5$	$4.6 \cdot 10^7$

Charged pions (on right in figure 7) can be produced in direct reaction at a rate larger than neutral pions only for  $T > 35$  MeV. The photon channel dominates.

#### IV. DISCUSSION AND CONCLUSIONS

We found that the production of  $\pi^0$  is the dominant coupling of electromagnetic radiation to heavy (hadronic) particles with  $m \gg T$ , and as we have here demonstrated that noticeable particle yields can be expected already at modest temperatures  $T \in [3, 10]$  MeV. In present day environment of 0.1 –1 J plasma lasting a few fs, our results suggest that we can expect integrated over space-time evolution of the EP<sup>3</sup> fireball a  $\pi^0$  yield at the limit of detectability. For  $T \rightarrow 15$  MeV the  $\pi^0$  production rate remains dominant and indeed very large, reaching the production rate  $R' \simeq 10^{15}[\text{MJ}^{-1}\text{fs}^{-1}]$ . Charge exchange reactions convert some of the neutral pions into charged

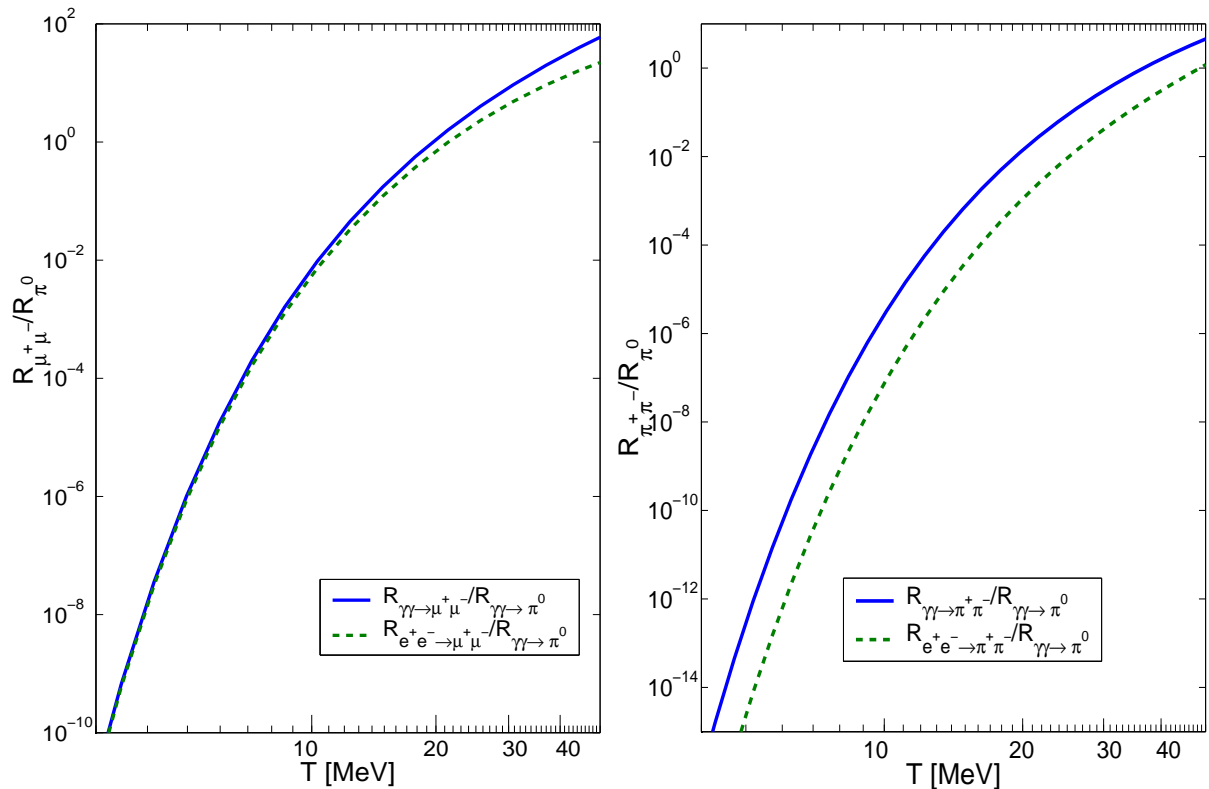


FIG. 7: On left: Muon and on right charged pion production rates in electromagnetic processes normalized by  $\pi^0$  production rate. Solid line (blue) for  $\gamma\gamma$ , dashed line (green) for  $e^+e^-$  induced process.

pions which are more easy to detect.

In this situation it is realistic to consider the possibility of forming a chemically equilibrated fireball with  $\pi^0, \pi^\pm, \mu^\pm$  in chemical abundance equilibrium. The heavy particles are produced in early stages when temperature reached is highest. Their abundance in the fireball follows the fireball expansion and cooling till their freeze-out, that is decoupling of population equation production rates. The particle yields are than given by the freeze-out conditions, specifically the chemical freeze-out temperature  $T_f$  and volume  $V_f$ , rather than the integral over the rate of production. In this situation the heavy particle yields become diagnostic tools of the freeze-out conditions, with the mechanisms of their formation being less accessible. However, one can avoid this condition by appropriate staging of fireball properties.

The present study has not covered, especially for low temperature range all the possible mechanisms, and we addressed some of these issues in the introduction. Here we note further that the production of heavy particles requires energies of the magnitude  $m/2$  and thus is due to collisions involving the (relatively speaking) far tails of a thermal particle distribution. If these tails fall off as a power law, instead of the Boltzmann exponential decay [19], a much greater yield of heavy particles could ensue. There could further be present a collective amplification to the production process e.g. by residual matter flows, capable to enhance the low temperature yields, or by collective plasma oscillations and inhomogeneities.

These are just some examples of many reasons to hope and expect a greater particle yield than we computed here in microscopic and controllable two particle reaction approach. This consideration, and our encouraging ‘conventional’ results suggest that the study of  $\pi^0$  formation in QED plasma is of considerable intrinsic interest. Our results provide a lower limit for rate of particle production and when folded with models of EP<sup>3</sup> fireball formation and evolution, final yield.

It is of some interest to note that the study of pions in QED plasma allows exploration of pion properties in electromagnetic medium. Specifically, recall that 1.2% fraction of  $\pi^0 \rightarrow e^+e^-\gamma$  decays, which implies that the associated processes such as  $e^+ + e^- \rightarrow \gamma + \pi_0$  are important. We cannot evaluate this process at present as it involves significant challenges in understanding of  $\pi_0$  off-mass shell ‘anomalous’ coupling to two photons.

The experimental environment we considered here should allow a detailed study of the properties of pions (and also muons) in a thermal background. There is considerable fundamental interest in the study of pion properties and specifically pion mass splitting in QED plasma at temperature  $T \gtrsim \Delta m$  and in presence of electromagnetic fields. We already have shown that due to quantum statistics effects, the effective in medium decay width of  $\pi^0$  differs from the free space value, see figure 2. In addition, modification of mass and decay width due to ambient medium influence on the pion internal structure is to be expected. Further we hope that the study of pions in the EP<sup>3</sup> fireball will contribute to the better understanding of the relatively large difference in mass between  $\pi^0$  and  $\pi^\pm$ . The relatively large size of the PE<sup>3</sup> environment should make such changes, albeit small, measurable.

The experimental study of  $\pi^0$  in QED plasma environment is not an easy task. Normally, one would think that the study of the  $\pi^0$  decay into two 67.5 MeV  $\gamma$  (+ thermal Doppler shift motion) produces a characteristic signature. However, the  $\pi^0$  decay is in time and also in location overlapping with the plasma formation and disintegration. The debris of the plasma, reaches any detection system at practically the same time instance as does the 67.5 MeV  $\gamma$ . The large amount of available radiation will disable the detectors. On the other hand we realize that the hard thermal component of the plasma, which leads to the production of  $\pi^0$  in the early fireball stage, is most attenuated by plasma dynamical expansion. Thus it seems possible to plan for the detection of  $\pi^0$  e.g. in a heavily shielded detection system.

The decay time of charged pions being 26 ns, and that of charged muons being 2.2  $\mu$ s it is possible to separate in time the plasma debris from the decay signal of these particles. Clearly, these heavy charged particles can be detected with much greater ease, also considering that the decay product of interest is charged. For this reason, we also have in depth considered all channels of production of charged pions and muons. Noting that practically all charged pions turn into muons, we have also compared the production rates of  $\pi^0$  with all heavy particles, see dot-dashed (green) line in figure 7. This comparison suggests that for plasmas at a temperature reaching  $T > 10$  MeV the production of final state muons will most probably be by far easier to detect. On the other hand for  $T < 5$  MeV it would seem that the yield difference in favor of  $\pi^0$  outweighs the detection system/efficiency loss considerations. Future work addressing non-conventional processes will show at how low  $T$  we can still expect observable heavy particle yields.

An effort to detect  $\pi^0$  directly is justified since we can learn about the properties of the plasma (lifespan, volume and temperature in early stages) e.g. from a comparative study of the  $\pi^0$  and  $\pi^\pm$  production. We have found that at about  $T > 16$  MeV, the pion charge exchange  $\pi^0\pi^0 \rightarrow \pi^+\pi^-$  reaction for chemically equilibrated  $\pi^0$  yield is faster than the natural  $\pi^0$  decay, and the chemical equilibration time constant, see the dot-dashed line in figure 5. Thus beyond this temperature the yield of charged pions can be expected to be in/near chemical equilibrium for a plasma which lives at, or above this temperature, for longer than 100 as.

In such an environment the yield of  $\pi^0$  is expected to be near chemical equilibrium, since the decay rate is compensated by the production rate, and, within 100 as, the chemical equilibrium yield is attained. Moreover, the thermal speed of produced  $\pi$  can be obtained from the nonrelativistic relation  $\frac{1}{2}m\langle v^2 \rangle = \frac{3}{2}T$ , thus  $\bar{v} \propto \sqrt{T}$  and, for  $T = 10$  MeV,  $\bar{v} \simeq 0.5c$ . This is nearly equal to the sound velocity of EP<sup>3</sup>,  $v_s \simeq c/\sqrt{3} = 0.58c$ . Thus the heavy  $\pi^0$  particles can be seen as co-moving with the expanding/exploding EP<sup>3</sup>, which completes the argument to justify their transient chemical equilibrium yield in this condition.

The global production yield of neutral and charged pions should thus allow the study of volume and temperature history of the QED plasma. More specifically, since with decreasing temperature, for  $T < 16$  MeV, there is a rapid increase of the relaxation time for the charge exchange process, there is a rather rapid drop of the charged pion yield below chemical equilibrium — we note that charge exchange equilibration time at  $T = 10$  MeV is a factor  $10^5$  longer. We note that the study of two pion correlations provides an independent measure of the source properties (HBT measurement).

The relaxation time of electromagnetic production of muon pairs wins over  $\pi^0$  relaxation time for  $T > 22$  MeV, see dashed line, red, in figure 5, the direct electromagnetic processes of charged pion production (thin green, solid line for  $\gamma\gamma \rightarrow \pi^+\pi^-$  and dashed, blue for  $e^+e^- \rightarrow \pi^+\pi^-$ ) remain sub-dominant. Thus for  $T > 22$  MeV we expect, following the same chain of arguments for muons as above for charged pions, a near chemical equilibrium yield. If the study of all these  $\pi^0, \pi^\pm, \mu^\pm$  yields, their spectra and even pion correlations were possible, considerable insight into  $e^-, e^+, \gamma$  plasma (EP<sup>3</sup>) plasma formation and dynamics at  $T < 25$  MeV can be achieved.

*Acknowledgments*

This research was supported by the DFG Cluster of Excellence: Munich Center for Advanced Photonics and by a grant from: the U.S. Department of Energy DE-FG02-04ER4131.

- 
- [1] T. Tajima and G. Mourou Phys. Rev. ST Accel. Beams **5**, 031301 (2002).
  - [2] T. Tajima, G. Mourou and S.V. Bulanov Phys. Mod. Phys. **78**, 309 (2006)
  - [3] M. H. Thoma, arXiv:0801.0956 [physics.plasm-ph].
  - [4] Baifei Shen and J. Meyer-ter-Vehn Phys. Rev. E **65**, 016405 (2001).
  - [5] See for example introduction in *Statistical Physics (Course of Theoretical Physics, Volume 5* by E M Lifshitz and L D Landau.
  - [6] M. H. Thoma, private communication.
  - [7] I. Kuznetsova, T. Kodama and J. Rafelski, “Chemical Equilibration Involving Decaying Particles at Finite Temperature ” in preparation.
  - [8] T. Biro and J. Zimanyi, Phys. Lett. B **113**, 6 (1982).
  - [9] J. Rafelski and B. Muller, Phys. Rev. Lett. **48**, 1066 (1982) [Erratum-ibid. **56**, 2334 (1986)].
  - [10] T. Matsui, B. Svetitsky and L. D. McLerran, Phys. Rev. D **34**, 783 (1986) [Erratum-ibid. D **37**, 844 (1988)].
  - [11] P. Koch, B. Muller and J. Rafelski, Phys. Rept. **142**, 167 (1986).
  - [12] B. L. Combridge, Nucl. Phys. B **151**, 429 (1979).
  - [13] M. Gluck, J. F. Owens and E. Reya, Phys. Rev. D **17**, 2324 (1978).
  - [14] J. Letessier and J. Rafelski, Camb. Monogr. Part. Phys. Nucl. Phys. Cosmol. **18**, 1 (2002).
  - [15] R. Kaminski, J. R. Pelaez and F. J. Yndurain, “The pion-pion scattering amplitude. III: Improving the analysis with forward dispersion relations and Roy equations,” arXiv:0710.1150 [hep-ph].
  - [16] H. Terazawa, Phys. Rev. D **51**, 954 (1995).
  - [17] G. J. Gounaris and J. J. Sakurai, Phys. Rev. Lett. **21**, 244 (1968).
  - [18] G. Mennessier, P. Minkowski, S. Narison and W. Ochs, arXiv:0707.4511 [hep-ph]. in proceedings of the *3rd High-Energy Physics International Conference In Madagascar (HEPMAD07)* 10-15 Sep 2007, Antananarivo, Madagascar; Proceedings URL: <http://www.slac.stanford.edu/econf/C0709107>
  - [19] T. S. Biro and A. Jakovac, Phys. Rev. Lett. **94**, 132302 (2005) [arXiv:hep-ph/0405202].